Individual node's contribution to the mesoscale of complex networks

Florian Klimm[1,2,3]**, Javier Borge-Holthoefer**[4]**, Niels Wessel**[1]**, Jürgen Kurths**[1,2,5,6] **and Gorka Zamora-López**[7,8]

[1] Department of Physics, Humboldt-Universität zu Berlin, Berlin, Germany
[2] Potsdam Institute for Climate Impact Research, Potsdam, Germany
[3] Doctoral Training Centre, University of Oxford, Oxford, United Kingdom
[4] Qatar Computing Research Institute, Doha, Qatar
[5] Institute for Complex Systems and Mathematical Biology, University of Aberdeen, Aberdeen, UK
[6] Department of Control Theory, Nizhny Novgorod State University, Nizhny Novgorod 603950, Russia
[7] Center for Brain and Cognition, Universitat Pompeu Fabra, Barcelona, Spain
[8] Department of Information and Communication Technologies, Universitat Pompeu Fabra, Barcelona, Spain
E-mail: gorka.zamora@ymail.com

Abstract

The analysis of complex networks is devoted to the statistical characterization of the topology of graphs at different scales of organization in order to understand their functionality. While the modular structure of networks has become an essential element to better apprehend their complexity, the efforts to characterize the mesoscale of networks have focused on the identification of the modules rather than describing the mesoscale in an informative manner. Here we propose a framework to characterize the position every node takes within the modular configuration of complex networks and to evaluate their function accordingly. For illustration, we apply this framework to a set of synthetic networks, empirical neural networks, and to the transcriptional regulatory network of the *Mycobacterium tuberculosis*. We find that the architecture of both neuronal and transcriptional networks are optimized for the processing of multisensory information with the coexistence of well-defined modules of specialized

components and the presence of hubs conveying information from and to the distinct functional domains.

Keywords: network metrics, community structure, neuronal networks, genetic regulatory networks

1. Introduction

The representation of real systems as complex networks has become a successful practice in the literature across different scientific disciplines: biology, technology, sociology, climatology, etc. [1–4]. Graph analysis allows us to describe the topological organization of the constituents of a multi-component system and uncover their functional implications. This is of particular relevance in physiology whose central aim is to understand the biological function of the observed anatomical structures [5]. For example, recent studies indicated that such networks are highly complex in terms of dynamic reorganization in multiple hierarchical levels [6], highlighting the necessity to treat the system in an integrative manner. Brain networks, both anatomical and functional, have properties supporting brains function [7–9]. There is also growing evidence of how alterations in connectivity lead to brain malfunction or disease, and vice versa [10].

There exist a wide variety of graph measures to explore the structural organization of networks across scales, from local node properties to global organization. The intermediate scale, the *mesoscale*, has also received significant attention through investigation of modular structures present in the majority of real networks. Most efforts have focused on the determination of the modules, a computational problem commonly referred as the *community detection problem* [11–14], rather than on describing the mesoscale itself in an informative manner. Besides community detection, the nodes of real networks are often classified into categories according to meta-information of the system. Geographically embedded networks such as power-grids, the internet or the airport transportation networks can be subdivided into countries or continents. Agents of social networks may be classified according to gender, race, age or any other categories found in social structures. The remaining challenge is then, once a classification is known that segregates nodes into groups, how to characterize the interrelations between them and the function every node takes.

The first sound investigation about the analysis of the roles of nodes in relation to the community structure happened in the framework of the social sciences [11, 15–17]. Using block-models they characterized the roles of cliques in the social structure, e.g. identifying the leaders of two opposing groups in a monastery. More recently, Guimerà and Amaral characterized the roles of nodes according to two parameters: an indicator of the hubness and a participation index assessing how distributed are the links of a node across communities [18, 19]. In another effort, Arenas and coauthors introduced a formalism to study the mesoscale of complex networks based on a dimensionallity reduction of the community structure [20].

In the present work we introduce a set of graph descriptors to characterize the position every node takes within the modular and hierarchical architecture of complex networks overcoming the limitations of previous approaches. We acknowledge that this characterization is a multidimensional problem and define parameters with a straightforward interpretation in terms of basic graph properties. Contrary to previous efforts, we also take into consideration the

fact that communities are often inhomogeneous and account for the likelihood of nodes to belong to each community depending on their sizes.

For illustration we apply our framework to a set of physiological networks. First, we investigate the neuronal network of the nematode *Caernohabditis elegans* and the anatomical connectivity between cortical regions in cats and humans. These are known to inherit a highly complex architecture due to the variety of information processes they host at multiple scales [21]. We use this representation of node's roles in order to show that the structure of neuronal networks is optimized to process information in a way that combines specialization and integration [22, 23]. Those are two features that coexist thanks to the combination of modular differentiation and highly interconnected hubs [24–26]. Finally, we study the transcriptional regulatory network of the *Mycobacterium tuberculosis* [27, 28] to gain understanding on the relationship between functional classes of genes. We find that from a regulatory perspective— following the top-down hierarchical chain of command—the network combines specialized groups of genes and a few hubs capable of regulating the network globally resembling the modular and hierarchical organization of neuronal and cortical networks.

2. Characterization of node's role in modular networks

The connectivity of a network of N nodes is encoded in its adjacency matrix $A = \{A_{ij}\}$ where $i, j = 1, \ldots, N$. $A_{ij} = 1$ if there exists a link connecting nodes i and j, and $A_{ij} = 0$ otherwise. The number of links in the network is $L = \frac{1}{2}\sum_{i,j=1}^{N} A_{ij}$. The degree of a node, k_i, is defined as the number of nodes it is connected to: $k_i = \sum_{j=1}^{N} A_{ij}$. Community detection methods find partitions of nodes that optimize the internal density within modules and minimize the number of connections between them. The usability of such mesoscale information has been shown for many different areas because the communities identified usually match functional subparts of the system. Applications include social networks such as collaboration networks between scientists [11] or biological systems, e.g. protein interaction structure [29]. For comprehensive reviews of current technical developments see [12, 30]. Here we will use the *Louvain* method [31, 32] to extract the partitioning. As with most community detection methods it tries to find a partition that optimizes the modularity quality function

$$Q = \frac{1}{4M}\sum_{ij}\left(A_{ij} - \frac{k_i k_j}{2M}\right)\delta_{c(i),c(j)}. \tag{1}$$

The modularity Q evaluates the goodness of a partition comparing the actual fraction of links falling within the modules to the expected fraction if links were distributed at random conserving the degrees of the nodes [33]. There is a wide range of community detection methods available, each with individual advantages and shortcomings [14]. In order to validate the usage of the *Louvain* algorithm we recalculated partitions with the *Radatools* software [34], which allows the usage of various algorithms in an iterative manner and obtained similar partitions. In particular, partition similarity was measured as normalized mutual information [35, 36], with values above 0.5 in all cases.

A partition $\mathcal{L}$ is a set of M disjoint sets. Given a partition nodes can occupy different topological positions as illustrated in figure 1. The challenge is thus to define adequate parameters that permit us to identify nodes playing those different roles.
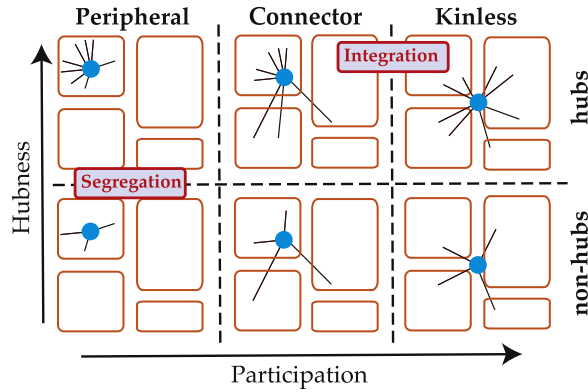
Figure 1. Illustration of the *topological roles* that nodes might occupy within the modular division of a network. Given a partition due to community detection or to external meta-information nodes can take different positions depending on how their links are distributed among communities. Following the nomenclature in [18], nodes only connected within their community might be regarded as *peripheral*, nodes with some connections with other modules as *connectors* and nodes with their links evenly distributed among modules as *kinless* because they could belong to any community. On the other hand, the global importance of the nodes can be quantified from their degree, classifying them into hubs or non-hubs. The combination of these two features, participation and hubness, gives rise to a wide spectrum of topological positions. In neuronal networks nodes with low participation fulfil the function of segregated information processing. Nodes with high participation and high hubness instead are integrating the information derived from the segregated modules.

2.1. Related work

Before presenting our formalism to characterize the roles of nodes in modular networks, we first review two previous efforts.

2.1.1. Mapping of functional roles.   The framework proposed in [18, 19] consists of a mapping of the nodes based on two parameters; one parameter evaluates the internal importance of the node within its module and the other one evaluates its external connectivity. The internal parameter, called the *within-module degree*, is defined as the z-score of the internal degree of the node:

$$z_i = \frac{k_i' - \langle k' \rangle}{\sigma'} \tag{2}$$

where k_{im} is the number of links the node makes with members of its community, $\langle k \rangle_m$ denotes the average internal degree of the nodes in the community and σ_m their standard deviation. The external parameter, the *participation coefficient*, quantifies how distributed are the links of a node among all the communities:

$$P_i = 1 - \sum_{m=1}^{M} \left(\frac{k_{im}}{k_i} \right)^2 . \tag{3}$$

$P_i = 0$ if all the links of a node fall in the same community and $P_i = 1$ if its links are uniformly distributed among all the modules. Following these two parameters, the nodes of a network can

be mapped into a z-P plane in which nodes of different roles occupy distinguished regions, similar to those illustrated in figure 1. This framework suffers from a few shortcomings that limit its application and the interpretation of the results obtained: (*i*) nodes are classified as hubs or non-hubs based exclusively on the information of their internal degrees when in the literature the term hub is associated with the degree to which a node, comprises the whole network. (*ii*) All communities are assumed to have identical statistical properties. For example, if two modules had different internal degree distributions their z_i nodes are evaluated over different statistical baselines. On the other hand, the formulation of the participation index assumes that all communities are of the same size. (*iii*) The largest value of P_i depends on the number of communities. In a partition with M communities the largest participation a node can take is $P_i = 1 - \frac{1}{M} < 1$ when according to [18], it should be $P_i = 1$. As a consequence P_i values across networks are only comparable if both networks contain the same number of communities.

2.1.2. Algebraic approach to characterize the modular skeleton. The approach introduced in [20] is based on the linear decomposition of the modular organization of a network. It accounts for the multidimensional nature of the problem to classify nodes. Given a partition $\mathcal{L}$ of the network into M communities, the *contribution matrix* **C** is defined as the number of links each node devotes to every community, $C_{is} = k_{is}$. The contribution matrix contains all the information of the modular structure and the challenge is to extract this information in a structured manner. This is achieved by application of singular value decomposition (SVD) to the **C** matrix and investigating its principal directions. In this representation every module has its own intrinsic direction $\tilde{\mathbf{e}}_\mathbf{s}$ in the M-dimensional space corresponding to the direction of those nodes that are only internally connected and make no external connections with other modules. The deviation of a node's projection $\tilde{\mathbf{n}}_\mathbf{i}$ from $\tilde{\mathbf{e}}_\mathbf{s}$ represents its tendency to connect with other modules. Equivalently, the deviation of the sum of a module's nodes projections $\tilde{\mathbf{m}}_\mathbf{s}$ represents the tendency of the module C_s to connect to other modules; $\tilde{\mathbf{m}}_\mathbf{s} = \tilde{\mathbf{e}}_\mathbf{s}$ only when the module is disconnected from the others. On the other hand, the scalar product of the modular projections $\tilde{\mathbf{m}}_\mathbf{s}$ reflects the relationships between modules allowing to investigate how modules are interrelated. Despite its elegance and its success to map the skeleton formed by the communities, the information for individual nodes is more difficult to extract and differentiate. As it usually happens with linear decomposition methods the interpretation of the optimal dimensions and their projections in terms of the natural parameters of the system is not trivial due to the mixture of information.

Altogether, we find that the functional mapping formalism lacks universal criteria and the parameters given by the algebraic approach are difficult to interpret node-wise. In the following we introduce a formalism based on four parameters, local and global, whose combination leads to a rich understanding of the roles that nodes play within modular networks. Our approach aims at being universal such that all networks are comparable within the same criteria. Additionally, it recognizes the fact that the probability of a node to connect to a community depends on the relative sizes of the communities.

2.2. Hubness index

One of the most important features found in real networks is the presence of highly connected nodes or hubs. Despite their importance a formal definition of hubness is missing; they are informally defined as '*those nodes with many more connections than others*'. The hallmark of

networks containing hubs, scale-free networks, possess a power-law degree distribution meaning that most nodes make only few links and a few nodes have many connections. The degrees of hubs is usually orders of magnitude larger than that of the averagely connected nodes. The within-module degree in equation (2) is intended to capture this notion of hubness by estimating the significance of a node's degree compared to that of its neighbours.

Now, we note a paradoxical behaviour in the hubs of scale-free networks: despite having much larger degrees than other nodes, hubs are only connected to a small fraction of the network. This happens because typically studied scale-free networks, both synthetic and real, are sparse. For example, in a scale-free network with $N = 100, 000$ nodes and exponent $\gamma = 3$ the most connected hubs are linked with only $2\%-5\%$ of all nodes. In contrast, many real networks are dense and therefore the loose definition of hubness above does not comply. The same applies to the internal connectivity of the modules which are, by definition, densely connected parts of a network. In dense (sub-)networks the mean degree is of the same order of magnitude as its size, $\langle k \rangle > \sim N$, and therefore the difference between the least and the most connected nodes is considerably reduced. Also, contrary to the hubs of scale-free networks, the hubs of dense networks are connected to a large fraction of the nodes. In dense networks it is usual to find hubs connected from 30% up to 70% of the network.

We find that for a measure of hubness to be universal it requires the assessment of the degrees under a common statistical baseline. The simplest choice to define the hubness index h_i of a node such that it is comparable across different (sub-)networks is to normalize the degree by the size of the (sub-)network, $h_i = \frac{k_i m}{N_m}$ [23]. However, this normalization does not account for the link densities. Therefore, we define the hubness as the comparison of the node's degree k_i with the degree distribution of an equivalent random graph of the same size N and density ρ. Since random graphs possess a narrow degree distribution around their mean degree $\langle k \rangle_R$, the more a node's degree deviates from the degree distribution of an equivalent random graph, the more reasonable it is to be considered as a hub. The mean degree of a random graph is $\langle k \rangle_R = (N-1)\rho$ and the standard deviation of its degree distribution is $\sigma_R = \sqrt{(N-1)\rho(1-\rho)}$ [1]. Constraining to networks without self-loops, we define the hubness index of a node in a network of size N and density ρ as:

$$h_i = \frac{k_i - \langle k \rangle_R}{\sigma_R} = \frac{k_i - (N-1)\rho}{\sqrt{(N-1)\,\rho\,(1-\rho)}}. \tag{4}$$

The hubness is negative for nodes with $k_i < \langle k \rangle_R$ allowing us to also identify outliers that are significantly less connected than expected from randomness. This index differs from the one defined in equation (2) in that all networks are compared to the same null-model—the random graph—instead of using the internal statistics of each network and of each community as a baseline for itself. This makes the index universal and the results for different networks and modules comparable.

Once the hubness index is defined we need to interpret the results and to identify its extremal values. In a random graph the degree of 99% of the nodes lies in the range bounded by $\langle k \rangle_R \pm 2.5\,\sigma_R$. In any network, nodes within this range shall not be considered outliers. The larger the h_i index grows above $2.5\,\sigma$ the more likely is the node a hub. The largest and smallest values that h_i can take depend on the size and the density of the network. In sparse networks it is not possible to find outliers on the negative side because $0 < \langle k \rangle \ll N$ and even disconnected nodes lie in the range of statistically expected degrees. However, there is plenty of room for
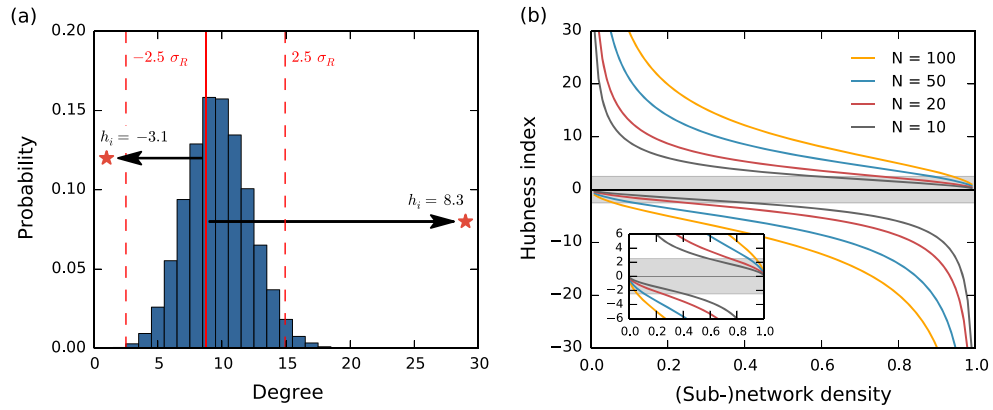
Figure 2. Dependence of the boundaries of hubness index on the size N and density ρ of the network. (a) Illustrative case for networks of $N = 30$ and $\rho = 0.25$. Due to the position of the degree distribution of random graphs with N and ρ, nodes can achieve different extremal values of significance. A node with the smallest degree $k_i = 1$ will take much smaller hubness than a node with the largest degree $k_i = 29$. (b) Upper and lower boundaries of hubness for networks of different size with increasing density. Inset shows the zoom near the thresholds $h_i \pm 2.5$.

some nodes to have a degree much larger than the mean and achieve high significance. Figure 2(a) illustrates this for a network with $N = 30$ and $\rho = 0.25$. A node with degree $k_i = 1$ gives $h_i = -3.1$ while a hub with $k_i = 29$ achieves $h_i = 8.3$. As the density increases the situation is reversed because $\langle k \rangle \to N$. The room for hubs decreases limited by the size of the network while from the bottom, occasional nodes with few connections become very significant. The hubness of a node with degree $k_i = 0$ is:

$$h^-(N, \rho) = -\frac{\langle k \rangle_R}{\sigma_R} = -\sqrt{\frac{(N-1)\,\rho}{1-\rho}} \tag{5}$$

and for a node with degree $k_i = N - 1$:

$$h^+(N, \rho) = \sqrt{\frac{(N-1)\,(1-\rho)}{\rho}} \;\; . \tag{6}$$

Equations (5) and (6) represent the lower and upper boundaries for the hubness index. In figure 2(b) the boundaries are shown for networks of different size and varying density. When networks are sparse the lower limit $h^- > -2.5\,\sigma$ regardless the size N and the upper bound tends to infinity. When networks are very dense, the opposite happens, the lower bound goes to $-\infty$ while there is no room for significant hubs because $h^+ < 2.5\,\sigma$. As highlighted in the inset, the limitations are stronger for smaller networks. For example, in networks of $N = 10$ there is no regime of density in which nodes with significant low and high degree can be found simultaneously.

From now on we will characterize nodes by two hubness values: the *global hubness* h^g is the hubness of the node in the network and the *local hubness* h^l is hubness within the community it belongs to. In this case N and ρ are replaced by the size and density of the community N' and ρ'.

2.3. Participation and dispersion indices

Given a partition $\mathcal{L}$ with M disjoint communities our aim is now to quantify how distributed is a node among them. In our framework we acknowledge that the contribution of a node to each community depends also on the size of the community. Imagine a network with only two communities, one of size $N_1 = 20$ and another of size $N_2 = 40$. A node devoting ten links to each of them is contributing more to the small community than to the large one and therefore, it is more likely to belong to the small community. We introduce the concept of *participation vector* $\boldsymbol{P_i}$ whose elements P_{im} represent the probability that node i belongs to community C_m, where $m = 1, 2, \ldots, M$. This probability is given by $P_{im} = \frac{k_{im}}{N_m}$ where N_m is the size of the community. Since we are only interested in the relative differences participation vectors are normalized such that $\sum_{m=1}^{M} P_{im} = 1$. Otherwise the norm of $\boldsymbol{P_i}$ would be proportional to the degree k_i but this information shall be disentangled and captured only by the hubness index. The vector of a node devoting all its links to the second community of a network with $M = 4$ communities is $\boldsymbol{P_i} = (0, 1, 0, 0)$ and for a node whose links are all equally likely distributed among the four communities, $\boldsymbol{P_i} = (\frac{1}{4}, \frac{1}{4}, \frac{1}{4}, \frac{1}{4})$.

Once the participation vectors have been computed for all nodes, we want to reduce that information into scalar values to quantify how distributed are the links of a node among all the communities. For consistency with previous definitions $p_i = 0$ if the node devotes all its links to a single community and $p_i = 1$ if its links are equally likely to be distributed among *all* the modules. Therefore we evaluate the standard deviation $\sigma(\boldsymbol{P_i})$ of the elements of the participation vector $\boldsymbol{P_i}$ and define the participation index as:

$$p_i = 1 - \frac{\sigma(\boldsymbol{P_i})}{\sigma_{max}(M)} = 1 - \frac{M}{\sqrt{M-1}}\,\sigma(\boldsymbol{P_i}). \tag{7}$$

The normalization factor accounts for the fact that the standard deviation of an M dimensional vector with all elements equal to zero but one is $\sigma_{max}(M) = \sqrt{M-1}\,/\,M$.

The larger its p_i the more difficult it is to classify the node into one and only one community. But for a node to be difficult to classify it is not necessary that it connects to all the communities. If a node is equally likely connected with only two of the communities, it is also difficult to classify. Such a node has for example a participation vector $\boldsymbol{P_i} = (0, \frac{1}{2}, 0, \frac{1}{2})$. To account for this information we define the dispersion of a node d_i equivalent to the participation index but considering only the non-zero entries of the participation vector:

$$d_i = 1 - \frac{\sigma(\boldsymbol{P_i'})}{\sigma_{max}(M')} = 1 - \frac{M'}{\sqrt{M'-1}}\sigma(\boldsymbol{P_i'}), \tag{8}$$

where $\boldsymbol{P_i'}$ is the subvector containing only the non-zero entries of $\boldsymbol{P_i}$, and M' its dimension. A node only connected within one community has $d_i = 0$ and a node equally likely connected among $M' \leqslant M$ has $d_i = 1$. We note that in general $d_i \geqslant p_i$ with the equality only happening when $M' = M$. The dispersion index shall be regarded as a measure of how difficult it is to classify a node into only one community and the participation index as the global reach of a node's links among all the communities.

We note also that not all combinations of dispersion and participation are possible. The highest difference between a node's d and p is reached when $M' = 2$ and follows:

$$p^+(d, M) = 1 - \sqrt{\frac{M}{M-1}\left[\left(\frac{2-d}{2}\right)^2 + \left(1 - \frac{2-d}{2}\right)^2 - \frac{1}{M}\right]}. \qquad (9)$$

In the following sections we apply the four indices here defined—local hubness, global hubness, dispersion and participation—to investigate the topological contribution nodes take in both synthetic and in empirical networks.

3. Application to synthetic networks

Now we apply the defined metrics to different synthetic network models to demonstrate their use. First we design a small graph to illustrate the variety of positions a node can take in modular networks. We compare the results to those obtained by the functional mapping and the algebraic framework summarized above. We then proceed with the analysis of random and scale-free graphs, and finally, we turn our attention to modular graphs.

3.1. An illustrative example graph

The graph in figure 3(a) consists of $N = 47$ nodes that are grouped into three modules. Each node's affiliation is represented by a red circle (community I), blue diamond (community II), or purple triangle (community III). The partitioning was derived using the Louvain method for community detection [31, 32]. Community III is the largest one with 23 nodes and I and II are equally sized with 12 nodes each. Communities have density 0.52, 0.20 and 0.29 respectively as summarized in table 1. Thus each community is distinct from the other two. We hand-picked seven nodes to illustrate the different roles that can be identified in the 4-dimensional space (h^g, h^l, p, d). Instead of showing all six possible relations we restrict ourselves to the three plots we find most informative: (h^l, h^g), (p_i, h^g) and (p_i, d_i) corresponding to figure 3(b)–(d). The participation vectors representing the probability of belonging to the communities I, II and III for the selected nodes are:

node	I	II	III
11	1	0	0
22	0	1	0
43	0	0	1
44	0.52	0.48	0
45	0.32	0.32	0.35
46	0.38	0.41	0.2
47	0.48	0	0.52

– Nodes (11) and (22) are connected only within their modules and their participation and dispersion are therefore $p = d = 0$; we call them *peripheral* nodes. Both are connected to five nodes in their communities and have a small global hubness $h^g < 0$. They are representative of *peripheral non-hubs*, see figure 1, which can functionally be identified with specialized or segregated function in the network. The examination of their local hubness shows a fundamental difference: (11) also shows $h^l < 0$ and does not fulfil a prominent position in its module since community I is dense but (22) is the node with highest internal degree in II, which is a sparse module and is therefore a local hub.
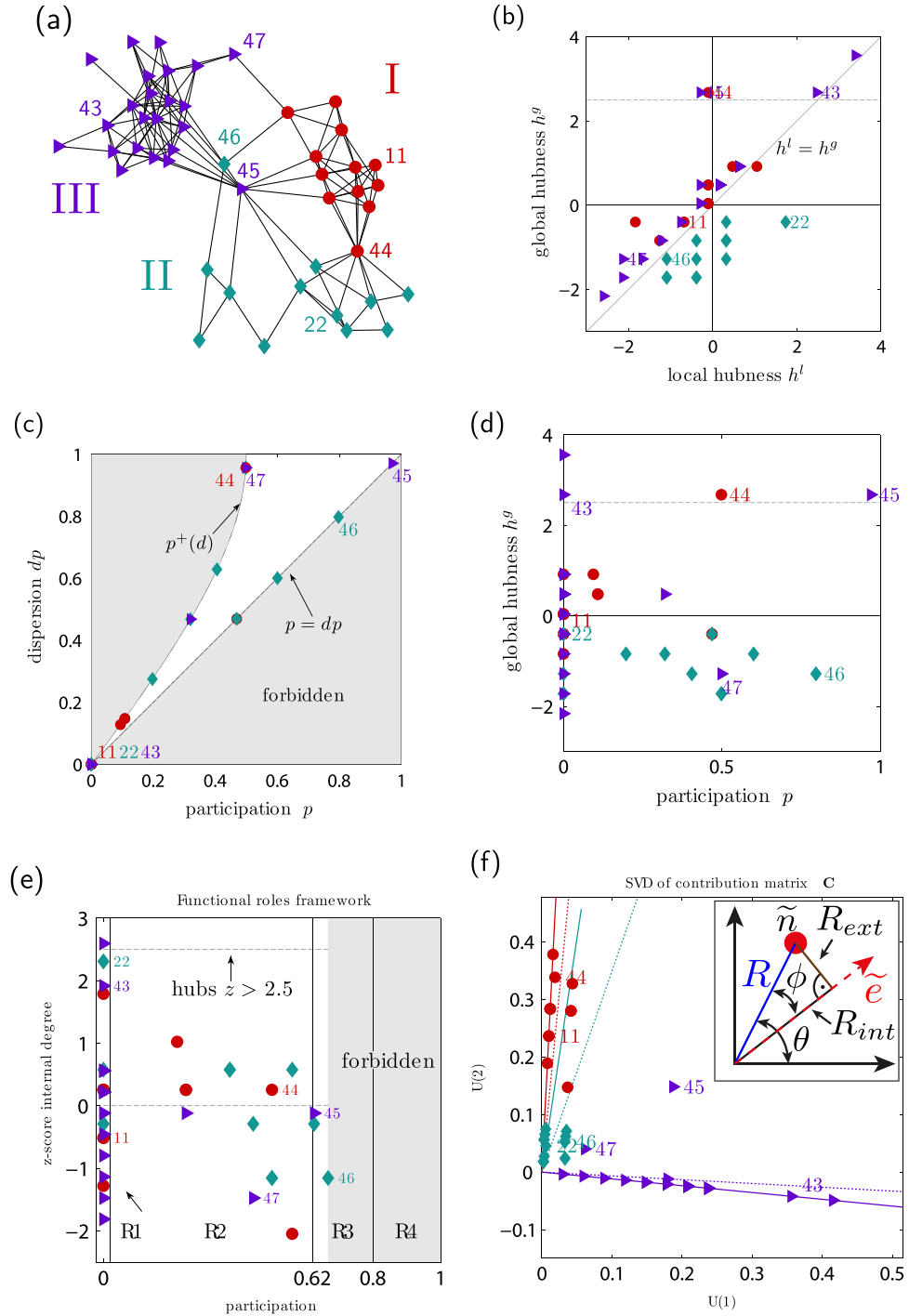
Figure 3. The exemplary graph consisting of three modules (red circles, blue diamonds and purple triangles) of sizes 12, 12, and 23 for demonstrating different roles nodes can have in the mesoscale structure of a network. The upper panels show the graph and 3 scatter plots of the metrics we defined: local hubness h^l, global hubness h^g, participation p, and dispersion d. Below you see the formerly introduced functional roles framework (participation and z-score internal degree) and the two leading dimensions U_1 and U_2 from the SVD of the contribute matrix **C**.

Table 1. Sizes, number of edges and densities of communities I, II, and III of the example graph shown in figure 3(a).

Community	size	edges	density
I	12	34	0.52
II	12	14	0.20
III	23	73	0.29

– Node (43) is also only connected within its module and its participation and dispersion are $p = d = 0$. Since it belongs to the largest community it is also one of the nodes with highest global hubness h^g. It is both a local and a global hub with no participation. It is characteristic of the rare *peripheral hub* category; see figure 1.

– Node (44) is a member of community II but devotes the same number of links, six, to community I. It is therefore hard to determine to which of the two communities it belongs. This results in a dispersion index $d \approx 1$. However, it makes no links with community III and has a reduced participation index of $p = 0.5$. This node cannot be considered as a kinless hub but it is a typical *connector hub*. The reduced participation however restricts the node's ability to integrate information from all parts of the network.

– Node (45) instead has the same number of neighbours but those are spread out amongst all three modules. It is a *kinless hub* with the ability to integrate on a global scale. Since it belongs to community III, which is densely connected, its local hubness is $h^l < 0$.

– Node (46) has only three neighbours but they are each in one of the three communities. Therefore (46) is neither locally nor globally a hub but its high participation makes it a kinless node that is located between all communities.

– Node (47) has two neighbours in its own community III and one in the community II which is half the size. Therefore it has almost equal likelihood to belong to any of the two communities and achieves a large dispersion value close to one. Its lack of connectivity to the community III reduces its participation index to $p \approx 0.5$; therefore we can classify this node as a *non-hub connector*.

In figure 3(e) the results for this graph are shown using the framework of the functional roles. Most of the nodes, including (11), (22) and (43) are classified as ultra-peripheral (R1) but none as hubs. Since only the internal degree is considered for the classification of nodes into hubs and non-hubs, node (22) is almost regarded as a hub but node (43) is assigned lower hubness despite being connected to more than twice the number of nodes as node (22). This misclassification is the result of assigning global hubness to local hubness and of a lack of normalization that accounts for the size and density of each community. On the other hand, the dependence of P_i on the number of communities, the accessibility to the region (R3) of connector hubs is reduced and to the region of kinless nodes (R4), forbidden.

The participation vector's reduction onto the leading two dimensions with the SVD is able to detect two main insights: a larger radius R stands for a mixture between higher degree/hubness and participation. The intramodular projection vector for each module (dashed lines) $\tilde{e}$ is close to the modular projection (solid lines) $\tilde{m}$ if the module is mostly internally connected. The projection on this vector gives for each node a measure of the number of neighbours in this particular module. The angular distance then is a measure of how strongly a node participates in each module. Node (45) for example has a large angular distance from all modular vectors since
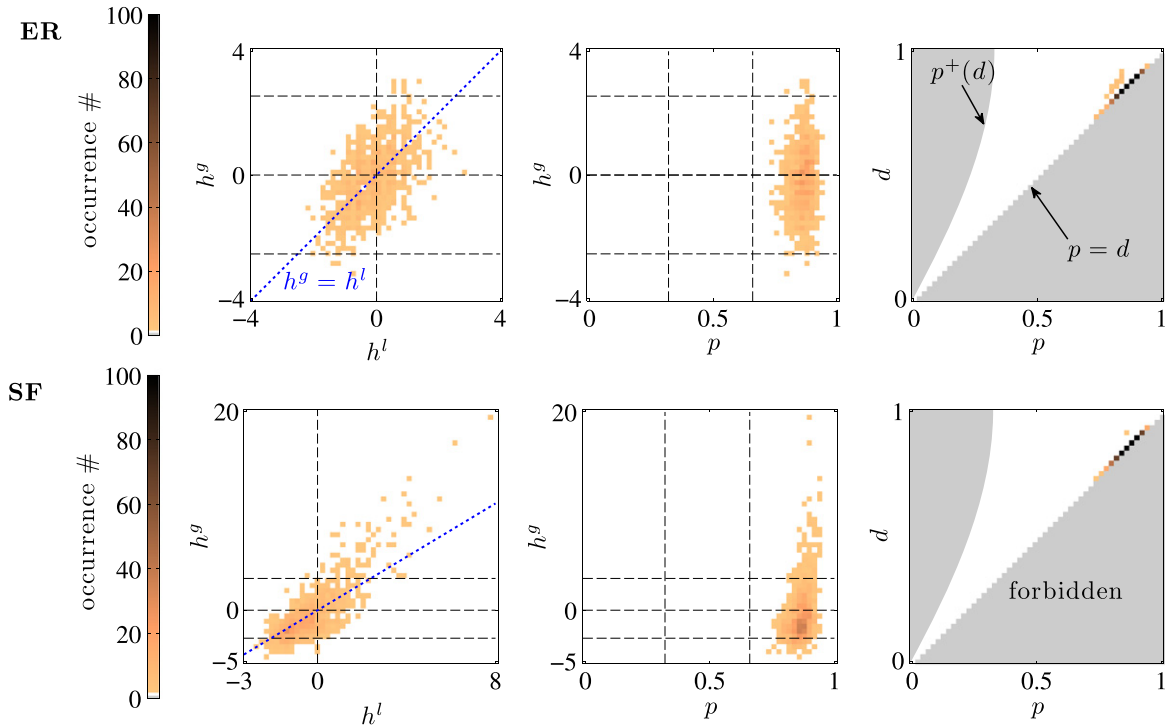
Figure 4. Density plots of mesoscale descriptors (global hubness h^g, local hubness h^g, participation p and dispersion d) for ER (upper panel) and SF (lower panel) networks: ER network with $N = 1000$ nodes and a density of $\rho = 0.1$, partitioned into $M = 9$ communities. SF of same size and density with a scale-free exponent of $\gamma \approx 3$, partitioned into 9 communities as well.

it is a kinless node. However the SVD is strongly dominated by the largest module III and modules I and II are almost not distinguishable from each other. Therefore the method, in its 2-dimensional representation, is not suited for our purposes.

We have seen that our approach is capable of detecting a wide variety of node roles in the mesoscale. However, the usage of four different metrics makes the illustration and interpretation a non-trivial task. Therefore we proceed with the illustration of the method applied to four artificial networks, followed by examples of biological networks. In the synthetic network examples we show results for a single realization since the number of communities usually differs from realization to realization. Still, the results remain general.

3.2. Random and scale-free graphs

We now analyze two fundamental network models: the Erőds-Renyi (ER) graph and the scale-free (SF) graph. These models lack intrinsic community structure and serve to illustrate the case in which the analysis of the mesoscale fails to return reasonable results due to the absence of structure in the mesoscale, or due to poor partitioning. Ensembles of ER and SF graphs of size $N = 1000$ nodes and density $\rho = 0.1$ were generated. The SF networks were created using the method introduced in [37] and they were tuned to follow a scale-free degree distribution $P(k) = k^{-\gamma}$ with $\gamma = 3$.

The upper panel of figure 4 shows the distribution, as density plots, of the four metrics across realizations for the ER graph partitioned into nine modules. Firstly we note that the distribution of both local and global hubness is rather small as expected. There is a correlated trend between both since nodes with a large number of neighbours inside their module are, in general, those with high number of neighbours in the whole network. The high values of participation p and dispersion d mean that all nodes have a significant number of neighbours in other modules. Mostly in all nine modules as indicated by the fact that most nodes lie on the diagonal $p = d$. Nodes directly above the diagonal are linked to eight modules. There are no peripheral nodes having neighbours only in their own community ($p = d = 0$). These observations indicate that the community structure found is very poor, as it is expected for ER graphs. The (p, h^g) plot is often useful to detect the global roles and functionality of the nodes since it closely resembles the classification framework illustrated in figure 1. Here we see that all nodes have a kinless contribution to all different modules due to the lack of structure at the mesoscale.

The results for the SF graph are very similar (lower panel of figure 4), especially in terms of participation and dispersion. This also demonstrates the lack of structure at the mesoscale in random SF graphs. The difference arises in the hubness indices which reach much higher values due to the heavy tailed degree distribution. In the (p, h^g) plot it is seen that all nodes are again kinless, now with a clear hub structure expanding vertically.

Summarizing we find that networks with no intrinsic community structure do not show a diversity of roles when analyzing their mesoscale. All nodes tend to be connected with all modules and have a high participation. The hubs are detectable in the SF case but they are not distinguishable in participation and dispersion from the other nodes.

3.3. Modular graphs

Now we discuss graphs with an intrinsic modular structure. We analyze two modular graphs models, both consisting of $N = 1000$ nodes that are grouped into four equally sized modules. Inside the modules pairs of nodes are connected with probability 0.3 and externally with probability 0.05. In the first model version all connections are created at random and we refer to it as the random modular (RM) graph. We also introduce a modified version in which the external links between modules are created following a preferential attachment rule. This leads to a centralized modular (CM) graph. Following the SF network generation method in [37], the nodes of each modules of size M_m are indexed as i ($i = 1, 2, ..., M_m$) and are assigned a weight $p_i = i^{-\alpha}$, where α is a control parameter in [0, 1]. When connecting two different modules, nodes from each module are selected with a probability proportional to their weight. The degree distribution of network generated with this method follows a power law with $\gamma = (1 + \alpha)/\alpha$. In this case, the hubs from the different modules become interconnected. This strong connection between the hub nodes is called a *rich-club* since it was first discovered in social networks accounting for the fact that rich people tend to gather in social clubs [38]. Its first sound quantification was introduced in the study of the topological structure of the internet [39] and later found also in neuronal networks [25, 40, 41]. This combination of characteristics, modular structure with centralized interconnectivity occur in neuronal networks and so we want to understand their influence on the mesoscale.

We note that the local and the global hubness are strongly correlated; see figure 5 plot (h^l, h^g), mainly because they reflect the internal degrees of the nodes. The small amount of
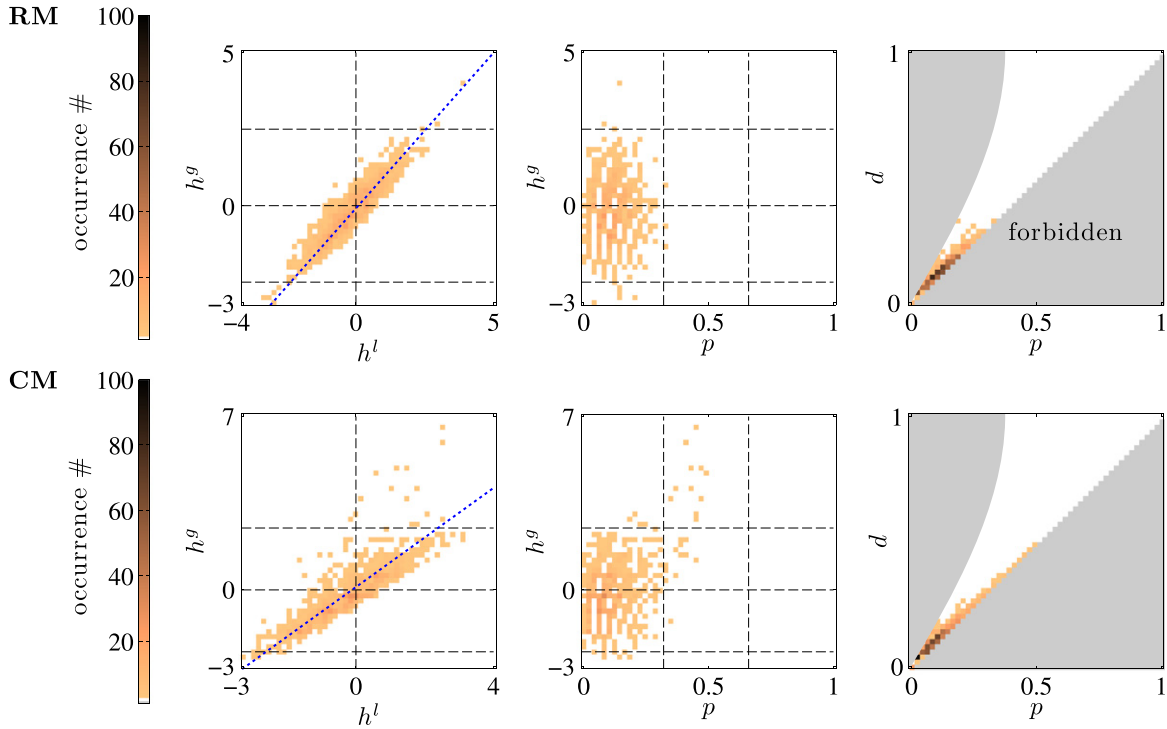
Figure 5. Density plots of mesoscale descriptors (global hubness h^g, local hubness h^g, participation p and dispersion d) for random modular (upper panel), and centralized modular graph (lower panel) Both networks consists of 5 equal sized modules with 200 nodes. Internally the modules are connected with a density of 30% and externally 0.5%. In the HMR both connections are completely random, in the HMC the external ones are created in a SF manner with $\gamma \approx 3$.

external connections per node has a weak influence on the relation ship between local and global hubness, especially in the RM model. Overall, due to the preferential attachment, global hubness takes larger values in the CM than in the RM model.

Focusing on the measures of participation and dispersion, plots (p, d), we find that their values are much lower than those observed before in ER and SF networks. This happens because the modules are well defined with most nodes densely connected inside their module and weakly connected externally. The communities are well defined in this case. However, only a small amount of nodes have neighbours in only one module and thus $p = d = 0$. This shows that the strong community structure does not go hand in hand with a strong core of nodes inside each module. In contrast the small amount of external edges is evenly distributed amongst all nodes and therefore almost all of them show external affiliations. In the RM graph there is no dependence between h^g and p. This occurs because external connections are created at random and therefore all nodes have the same probability of connecting to other modules. The (p, h^g) plot for the CM model is very similar but the hubs clearly stand out—they have larger hubness and participation. In the (p, d)-plane, the hubs lie on the $p = d$ line because they connect with the four modules. Due to this centralization non-hub nodes receive fewer external links and see their participation lessened.

In real networks the community organization happens as the consequence of functionally related nodes being gathered together. In this manner groups of specialized function are

segregated, restricting the influence of nodes with different function on them. In the RM model the communication between the modules is limited due to the overall small dispersion. In the CM model the hubs connect with all the modules allowing them to integrate information from the distinct functional groups. In the following we analyze neural networks for which the ability to maintain a balance between the amount of segregation between functional groups and an efficient communication between them is fundamental for their optimal working.

4. Segregation and integration in empirical neuronal networks

In this section we study the mesoscale structure of real neuronal networks. We start with the fully mapped neuronal network of the nematode *Caenorhaditis elegans* and finish with the corticocortical connectivites from the cat and human brains. Previous studies have shown that these networks combine the existence of modules of functionally related neurons or regions with the presence of highly connected hubs [22, 23, 25]. The segregation into modules allows the brain to handle information from different sensory systems in a temporal and spatial parallel manner. However, the brain needs to combine—integrate—the multisensory information in order to create a comprehensive understanding of the environment. It is believed that the neural hubs aid in the integration because of their capacity to reach information from different sensory systems.

The *C. elegans* is widely used as a model organism in neuroscience since its whole connectome has been mapped [42]. Here we use the data from [43] in a binary form without distinguishing between gap junctions and chemical synapses. The network consists of 302 neurons but we restrict ourselves to the largest connected component of 279 nodes and a total of 2285 edges [44]. Despite the worm's small size (1 mm long) and simple nervous system it shows a broad range of non-trivial behaviour, including chemotaxis and mating [45]. We use a Louvain-partition of the network in four communities of 50, 51, 88 and 90 neurons each. When analyzing the roles of nodes in the network, see results in figure 6, we find some characteristics similar to those observed in the synthetic networks and other distinctive properties. Similar to SF networks the *C. elegans* shows broad hubness distributions with local and global hubness being highly correlated. The range of h^g is larger than that of h^l indicating that the hubs might form a rich club. On the other hand, many nodes have significant negative hubness. The participation and the global hubness are correlated in this case. Non-hubs have low participation and hubs have high participation. Altogether these observations clearly reflect the modular and hierarchical organization of the network consisting of well defined communities (as shown by the large amount of nodes with negative hubness and very low participation) with the interconnections centralized by a set of global hubs forming a rich-club (hubs are both locally and globally hubs, and they have participation close to $p = 1$). In the (p, d) we appreciate that many nodes escape the $p = d$ line and take larger values of dispersion than of participation. This behaviour, not observed in the synthetic network models, is typical of connector nodes which have dispersed connectivity but do not connect with all the communities.

The nervous system of the *C. elegans* is subdivided into two main organizational parts. A small 'proto-brain' located in the pharynx and the rest of the neurons are symmetrically arranged, left and right, along the ventral cord. We also detect this bilateral symmetry in the pairwise occurrence of almost identical hubness and participation.
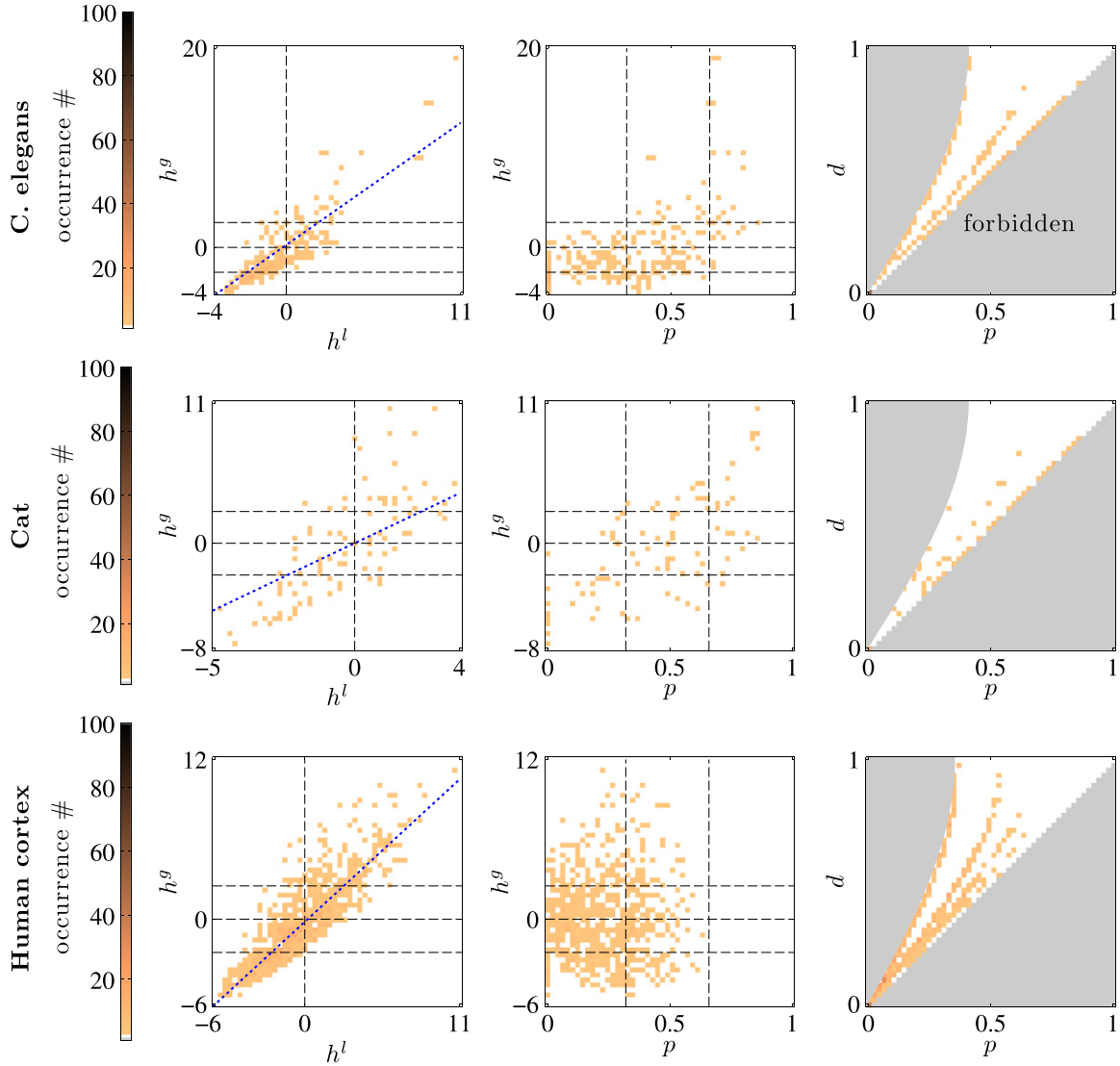
Figure 6. Density plots of mesoscale descriptors (global hubness h^g, local hubness h^g, participation p and dispersion d) for *C. elegans* neuronal network (upper panel), cat cortex data (middle panel) and human cortex connectivity data (lower panel).

The corticocortical connectivity of cats has been recently investigated to understand the relation between structure and function in the brains of higher organisms. The database used here is a combination of various published datasets [46]. We use a version into $N = 95$ cortical regions interconnected with $L = 1829$ white matter fibers. Here, we consider them undirected and unweighted. We use the Louvain partition into four modules of sizes 24, 21, 23 and 27. The analysis of the mesoscale reveals very similar data to that found for the *C. elegans* despite being only a third of the size and much more dense; $\rho_{cat} \approx 41\%$ and $\rho_{eleg} \approx 6\%$. Global and local hubness are correlated with h^g achieving again larger values than h^l. Global hubness and participation are also correlated. The non-hubs tend to have low participation indicating that they are tightly connected inside their communities. The hubs, on the contrary, have large participation showing that they are well connected with all the four communities. In the *(p, d)*
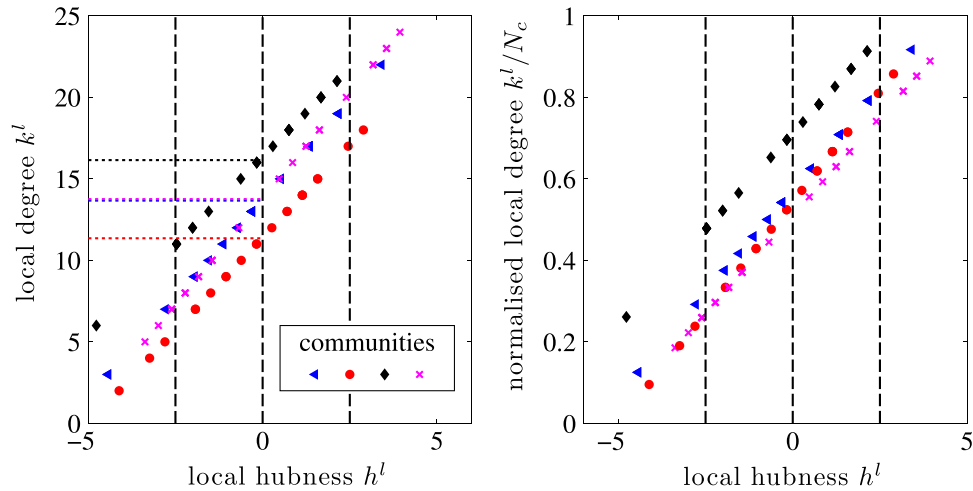
Figure 7. Local hubness h^l against local degree k^l (left panel) and normalized local degree k^l/N_c (right panel) for cat network. Nodes' affiliations to one of the four communities are shown as blue triangles, red circles, black diamonds and magenta crosses. Since the hubness takes into account the density of each module the determination of the local hubs is not equivalent: the node of the red community with the highest local degree has only moderate $k^l = 19$ and would therefore not be identified as a local hub since many nodes of other modules have a higher internal degree. However, the local hubness correctly identifies it as a local hub with $h^l \approx 3$. The vertical dashed line indicates $h^l = \{-2.5, 0, 2.5\}$ and thus horizontal dotted lines in the left panel are the mean local degree for each module.

plot we see, in contrast to the case in the *C. elegans*, that only few nodes reach $p_{max}(d)$, values that are reached for nodes that connect to only two modules.

For the human brain anatomical connectivity we used data first discussed in [47]. The connectivity is derived from non-invasive diffusion MRI able to detect white matter tracts that crisscross the human brain. We work with a binary adjacency matrix of a parcellation into $N = 994$ brain regions, after eliminating four isolated nodes, interconnected by $L = 13520$ white matter tracts. The network is partitioned into six modules of sizes 177, 143, 104, 156, 155 and 259. In the corresponding plots of figure 6 we can clearly detect again the presence of hubs. In contrast to the observations of the two previous networks, in this case the hubs only show intermediate values of participation as observed in the (p, h^g) plot. The majority of nodes show a very low hubness and also very low participation indicating a well-defined modular organization as in the networks of the *C. elegans* and of the cat. The lack of a high participation necessary for integration is a very interesting discrepancy with the other networks. One possible explanation for this difference might be the known limitation of tractography methods to recover long-range fiber tracts, especially those crossing through the *corpus callosum* from one brain hemisphere to the other. This limitation could have reduced the number of connections in the data between the homologous hubs in both hemispheres and let their participation appear diminished.

Finally, we demonstrate the advantage of the hubness measure over the simple degree. In figure 7 we show the local hubness h^l against the local degree k^l, also known as internal degree, for the neuronal network of the cat. By construction, the data for each module follows a strictly linear dependency. Nodes with $h^l = 0$ have mean internal degree of the module. Thresholding

the degree from the top to identify local hubs would favour nodes of the black and magenta communities. No node of the red community might be classified as a local hub. Normalizing the internal degree by the size of the community N_c does not correct the problem either, since the hubness of the nodes in the densest community would be overrepresented. Black is the densest community here. The definition of hubness here introduced adequately corrects for both size and density factors.

Summarizing we can state that the analysis of different topological roles that nodes can play inside the mesoscale structure of a network can give valuable insights in the structure and functionality of neuronal networks: we are able to link the functional task of information integration with the structural of connector and kinless hubs. On the other side the segregated information processing can only be achieved by nodes that are peripheral with sparse connectivity to other modules. Both structural properties are present in the three neuronal networks we analyzed. In particular we highlight the striking similarities in the structure of the *C. elegans* and the cat despite being two networks of very different scales.

5. Transcriptional network of *Mycobacterium tuberculosis*

As a last example, we study the mesoscale of the transcriptional regulatory (TR) network of the *Mycobacterium tuberculosis*. The network is the result of a collation of publicly available sources compiled in [27]. Building upon the TR network collected in [28], it was extended with new experimental information available from as many as 31 different publications. The final system contains 1624 nodes (genes) and 3212 links. We ignored the self-loops. The topology of the network is close to a directed tree with 894 (55%) nodes receiving only one link from a small set of 82 (5%) regulatory genes. Of the regulator genes, 41 of them receive no input links and are therefore unregulated. The other 41 receive and project links playing a transitive role; they are both regulated and regulators. The differences in the degree distributions between the output and the input links are very significant. The largest output degree found is 296 and the largest input degree is 12.

Following information on their reported function the genes can be classified into categories of genes involved in diverse tasks, e.g. lipid metabolism, cell wall control and respiration. Table 2 summarizes the categories applied in the 'TubercuList' database [48]. Note that the function of some of the genes is still unknown and they are classified separately. A particularity of this classification is that genes with regulatory capacity are grouped together independently of the concrete function they control. Therefore most regulatory genes are found in category IX with some exceptions, especially in I and III. The rest of categories only, or almost only, contain regulated genes.

For illustrative purposes and due to its biological relevance, in this example we consider this partition in ten functional categories based on meta-information of the system instead of performing an automated community detection of the network. We apply the analytical tools introduced in this paper to identify the place every gene takes in this functional partition. As the network is directed, we investigate the roles in both directions. Analysis in the natural direction of the information flow allows us to identify the most influential genes that regulate other genes across functionalities. The analysis in the reversed direction, transposing the adjacency matrix, permits us to find genes that are responsive to multicontextual cues from environmental signals.
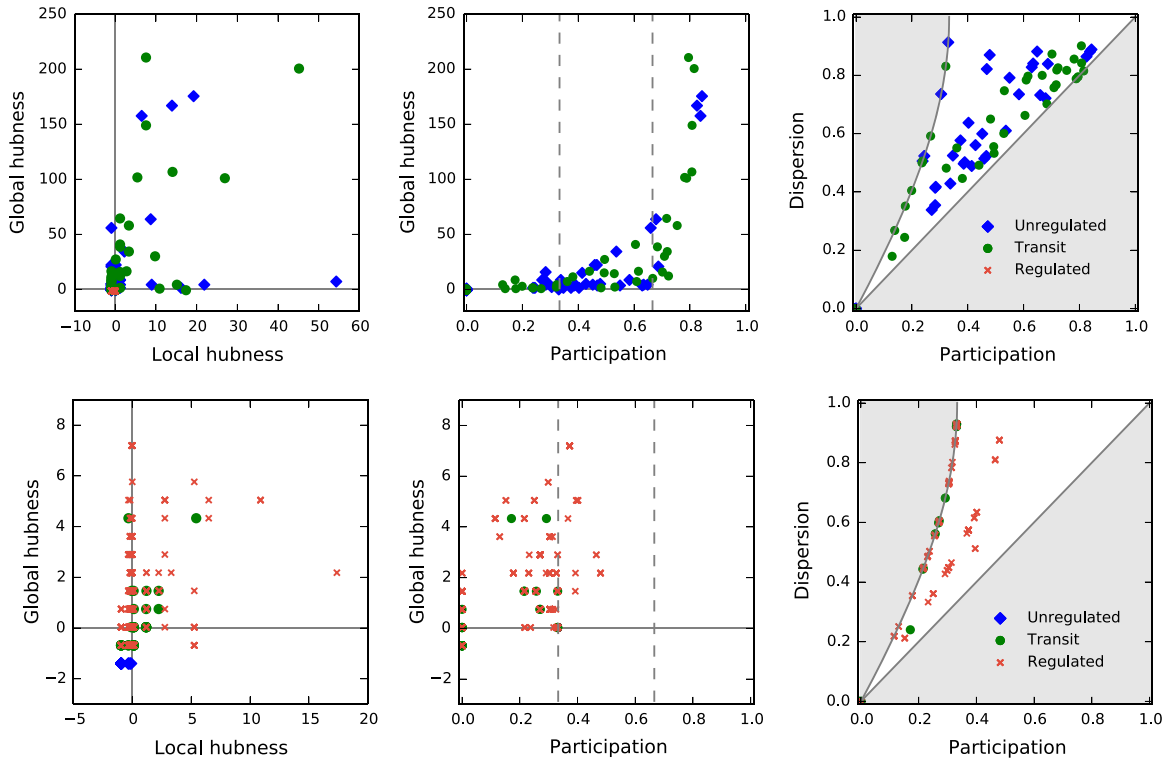
Figure 8. Analysis of functional roles of the regulatory transcription network of *Mycobacterium tuberculosis*. Top panels analysis of the output connectivity and bottom analysis for the input connectivity.

Table 2. Functional categories of the genes in the *Mycobacterium tuberculosis* according to their behavioural function as indicated in the 'TubercuList' database [48]. N_m refers to the size of the category and n_{in} and n_{out} the number of genes in the category with at least one input or output link respectively.

#	Description	N_m	n_{in}	n_{out}
I	virulence, detoxification, adaptation	87	85	5
II	lipid metabolism	131	131	0
III	information pathways	130	125	13
IV	cell wall and cell processes	305	305	1
V	insertion seqs and phages	38	38	0
VI	PPE/PE (polymorphic genes)	67	67	0
VII	interm. metabolism and respiration	387	385	2
VIII	unknown	4	4	0
IX	regulatory proteins	112	81	59
X	conserved hypotheticals	363	362	2

The results are shown in figure 8. Top panels are for the natural direction and lower panels for the analysis in the reversed direction. Several differences are appreciated between the results in the two directions. First, due to the distinct degree distributions, the hubness index achieved in the output direction is much larger than the one achieved in the input direction. There is no apparent correlation between global and local hubness. The main difference between the input

and the output direction happens when considering the participation. In the output direction there is a clear trend that non-hubs are peripheral (low participation) and hubs are kinless (high participation). This trend was also found in the cortical networks as a signature of their modular organization with a centralized hierarchy. In the input direction, however, this relation does not exist and no gene has a participation index larger than 0.5. Therefore, in the input direction there are no genes with full integrator capacity although there are connector nodes. This behaviour is to be expected since, as pointed out above, by construction of the functional categories most of the genes with regulatory capacities have been gathered in one single category. Nevertheless, the large dispersion values achieved by many genes demonstrates that a considerable number of them are co-regulated by genes in a different functional category and they could perform partial integration of information. 369 genes receive input from two categories, 42 genes from 3, and two of them receive input from four.

With $h^g > 100$ and $p > 0.75$ we find ten kinless hubs in the output direction: '*sigE*', '*sigB*', '*sigF*', '*sigG*', '*regX3*', '*mprA*', '*ideR*', '*crp*', '*phoP*' and '*Rv0348*'. The first four are members of Category I and the rest are regulatory genes from Category IX. Apart from '*sigE*' and '*sigB*', which are known to be involved in the heat-shock response, the particular function of the others is rather unclear according to the TubercuList database. Probably, the reason for their uncertain executive function is the fact they are able to control a variety of processes of different categories. In the input direction, we find nine connector genes with $p > 0.4$: '*hsp*', '*dnaK*', '*grpE*', '*dnaJ1*', '*grcC2*', *Rv0991c*', '*Rv0250c*', '*Rv0990c*' and '*Rv0992c*'. The first four belong to Category I and are related by behaviour in stress conditions: involved in heat-stress management and in the stimulation of ATPase activity. The rest are classified in Category X and are of unknown function.

We have found that the top-down regulation of the *Mycobacterium tuberculosis* follows a well-defined modular and hierarchical architecture. Although the executive function of hub genes has been reported in previous analyses of the network [27, 28], we have shown that these control many different functional domains instead of restricting their influence to particular categories. On the other hand, we have found that many genes are co-regulated by different functional categories although no gene seems to have global integrative properties.

6. Summary and discussion

In the present paper we have introduced measures to uncover the contribution that individual nodes make in modular networks or in networks with an *a priori* classification due to meta-information of the system. We have proposed four descriptors that help to map every node's contribution. On the one hand, local and global hubness indices parametrize the relevance of nodes locally within their community and globally on the whole network. On the other hand, we have proposed measures to evaluate how distributed are the links of a node among the communities. For that we have introduced participation vectors representing the likelihood of nodes to belong to each community; these account for inhomogenous relative sizes of the communities. Information in the participation vectors is reduced to two scalar indices. The dispersion index characterizes how difficult it is to classify a node in one and only one community and the participation index indicates how uniformly the links of a node are distributed among *all* the communities.

We have illustrated the use of the measures applying them to both synthetic and empirical networks. The example graph in figure 3 has been designed to contain nodes playing many different roles. In comparison with the results from previously defined frameworks, we show that only ours is able to distinguish the richness of roles that nodes take. Results in random and scale-free networks on the one hand, and in modular networks on the other hand, show fundamental differences between them. These examples demonstrate how the outcome of the participation and dispersion indices differ when the community structure is well-defined or not.

Analysis of empirical neuronal data has shown that our method is able to detect mesoscale features that are important to the information processing of those structures: on the one side a strong community structure is indicated by the presence of many nodes with very low participation values. These are the sites of segregated information processing. On the other side the hub structure is similar to a SF network organization. Importantly those hubs are connector or kinless hubs, showing that they are able to access information from all the different modules in order to combine and integrate it. The coexistence of integration and segregation is fundamental for the successful handling of information from multisensory input [23, 49–52].

Recently it has been shown that physiological networks arizing from sleep monitoring indicate the coexistence of several different forms of interaction [53]. The most appropriate formulation of such networks would be a multiplex-network [54] and extension of the tools derived here to such frameworks is feasible. However, in the mono-layer formation derived here, introducing multi-links between pairs of hubs from different modules would increase their ability to integrate information. Finally, we have found the same fundamental modular and hierarchical organization in the transcriptional regulatory network of the *Mycobacterium tuberculosis* as the one in neuronal networks, especially regarding the top-down regulatory direction, with well-defined modules and few hub genes capable of regulating genes of all functional domains. In the opposite direction, this structure is not so clear probably due to the construction of the functional categories. Still, we find many genes that are co-regulated by different functional domains. We have also observed that the specific biological function of the genes with large participation is very often still unknown or rather unclear. We find that the participation of those genes in multiple functional domains complicate their classification into one domain. As in neuroscience, understanding the purpose of specialized components is easier than recognizing the function of those components responsive to multi-contextual stimuli. The graph-analytical tools provided in the present paper allow us to explore the relations between functional domains of networked systems and clarify the responsibility of each component.

6.1. Comparison with previous approaches

The framework here proposed builds upon previous efforts to characterize the roles that nodes take in modular networks: the functional roles framework introduced in Guimerá and Amaral [18, 19] and the SVD approach by Arenas *et al* [20]. A common limitation of the two frameworks is that both assume all communities to be of the same size. While this is a reasonable approximation for large networks containing several large and near-to-homogeneous communities, many real networks are small or contain inhomogeneous communities.

Here, we have taken a probabilistic approach and evaluated the likelihood of a node to belong to a community that depends not only on the degree of the node but also on the size of the community. Stacking our participation vectors would lead to a matrix similar to the contribution matrix which would additionally account for the inhomogeneity of communities.

We have also proposed a measure of hubness that is consistent with the common and original understanding of hubs, say, that the degree of hubs in scale-free networks largely deviates from the expected, narrow degree distribution of random graphs. We have defined the hubness of a node as the difference between its degree and the typical degree distribution in equivalent random graphs. This definition allows us to compare the results out of different networks under a common statistical baseline. Additionally, we have shown that the hubness is bounded by finite-size effects depending on the size and on the density of the (sub-)networks.

6.2. Outlook

Future challenges of the formalism are its application to weighted or signed networks. From a technical point of view, we note the potential of participation vectors to improve community detection methods because they are ideal tools to identify misclassified nodes. This information can be used to switch nodes accordingly until the partition minimizing the number of misclassified nodes is reached. From a practical point of view, we foresee the interest of applying our formalism to multiplex and to multilayer networks. Our measures would allow one to one characterize the importance of nodes in relation to the different slices of the network in a statistically qualified way. We expect these tools to aid in uncovering general principles of organization in biological networks as the modular and hierarchical relations we found here for neural and transcriptional networks. In order to further analyze hierarchical organization recent multi-resolution community detection methods can be applied that return optimal partitions at different levels of mesoscale [55, 56]. For three of the discussed networks, *C. elegans* [57], human cortex connectivity [58] and *Mycobacterium tuberculosis* [59] such multiresolution approaches have been undertaken and the evaluation and discussion of the roles of nodes across scales will be a challenging and interesting task. Also, as observed for the transcriptional network of the *Mycobacterium tuberculosis* analyzed here, the function of many genes is still an enigma even for rather simple and small organisms, especially the function of those genes involved in multi-contextual processes. The examination of the individual gene's topological position within its network can largely help understand its purpose and to create predictions about its function that are experimentally testable *a posteriori*.

Acknowledgements

References

[1] Newman M E J 2010 *Networks: An Introduction* (Oxford: Oxford University Press)
[2] Bullmore Ed and Sporns O 2009 Complex brain networks: graph theoretical analysis of structural and functional systems *Nat. Rev. Neurosci.* **10** 186–98

[3] Junker B H and Schreiber F 2008 *Analysis of Biological Networks* volume 2 (Hoboken, NJ: Wiley)

[4] Donges J F, Zou Y, Marwan N and Kurths J 2009 Complex networks in climate dynamics *Eur. Phys. J. Spec. Top.* **174** 157–79

[5] Bashan A, Bartsch R P, Kantelhardt J W, Havlin S and Ivanov P Ch 2012 Network physiology reveals relations between network topology and physiological function *Nat. commun.* **3** 702

[6] Ivanov P C and Bartsch R P 2014 Network physiology: mapping interactions between networks of physiologic networks *Networks of Networks: The Last Frontier of Complexity* (New York: Springer) pp 203–22

[7] van den Heuvel M P and Hulshoff Pol H E 2010 Exploring the brain network: a review on resting-state fmri functional connectivity *Eur. Neuropsychopharmacology* **20** 519–34

[8] Meunier D, Lambiotte R and Bullmore E 2010 Modular and hierarchically modular organization of brain networks *Fronti. Neurosc.* **4**

[9] Bullmore E and Sporns O 2012 The economy of brain network organization *Nat. Rev. Neurosci.* **13** 336–49

[10] Bassett D S and Bullmore E 2009 Human brain networks in health and disease *Curr. Opin. Neurology* **22** 340

[11] Girvan M and Newman M E J 2002 Community structure in social and biological networks *Proc. Natl. Acad. Sci. India* **99** 7821–6

[12] Fortunato S 2010 Community detection in graphs *Phys. Rep.* **486** 174–75

[13] Danon L, Diaz-Guilera A, Duch J and Arenas A 2005 Comparing community structure identification *J. Stat. Mech.* **2005** P09008

[14] Lancichinetti A and Fortunato S 2009 Community detection algorithms: a comparative analysis *Phys. Rev.* E **80** 056117

[15] White H C, Boorman S A and Breiger R L 1976 Social structure from multiple networks. I. Blockmodels of roles and positions *Am. J. Sociol.* **81** 730–80

[16] Boorman S A and White H C 1976 Social structure from multiple networks. II. Role structures *Am. J. Sociol.* **81** 1384–446

[17] Lorrain F and White H C 1971 Structural equivalence of individuals in social networks *J. Math. sociol.* **1** 49–80

[18] Guimera R and Amaral L A N 2005 Cartography of complex networks: modules and universal roles *J. Stat. Mech.: Theory Experiment* **2005** P02001

[19] Guimera R and Amaral L A N 2005 Functional cartography of complex metabolic networks *Nature* **433** 895–900

[20] Arenas A, Borge-Holthoefer J, Gómez S and Zamora-López G 2010 Optimal map of the modular structure of complex networks *New J. Phys.* **12** 053009

[21] Klimm F, Bassett D S, Carlson J M and Mucha P J 2014 Resolving structural variability in network models and the brain *PLoS Comput. Biol.* **10** e1003491

[22] Sporns O and Tononi G 2001 Classes of network connectivity and dynamics *Complexity* **7** 28–38

[23] Zamora-López G, Zhou C and Kurths J 2011 Exploring brain function from anatomical connectivity *Front. neurosci.* **5**

[24] Sporns O 2013 Network attributes for segregation and integration in the human brain *Curr. Opin. neurobiol.* **23** 162–71

[25] Zamora-López G, Zhou C Z and Kurths J 2010 Cortical hubs form a module for multisensory integration on top of the hierarchy of cortical networks *Front. Neuroinform.* **4** 1

[26] Sporns O, Honey C J and Kötter R 2007 Identification and classification of hubs in brain networks *PloS ONE* **2** e1049

[27] Sanz J, Navarro J, Arbués A, Martín C, Marijuán P C and Moreno Y 2011 The transcriptional regulatory network of Mycobacterium tuberculosis *PLoS ONE* **6** e22178

[28] Balázsi G, Heath A P, Shi L and Gennaro M L 2008 The temporal response of the Mycobacterium tuberculosis gene regulatory network during growth arrest *Mol. Syst. Biol.* **4** 225

[29] Lewis A, Jones N, Porter M A and Deane C 2010 The function of communities in protein interaction networks *BMC Syst. Biol.* **4** 100

[30] Porter M A, Onnela J-P and Mucha P J 2009 Communities in networks *Not. Am. Math. Soc.* **56** 1082–97

[31] Blondel V D, Guillaume J-L, Lambiotte R and Lefebvre E 2008 Fast unfolding of communities in large networks *J Stat. Mech.: Theory Experiment* **2008** P10008

[32] Jutla I S, Jeub L G S and Mucha P J 2011-2012 A generalized louvain method for community detection implemented in matlab (http://netwiki.amath.unc.edu/GenLouvain)

[33] Newman M E J 2006 Modularity and community structure in networks *Proc. Nati. Acad. Sci.* **103** 8577–82

[34] Gomez S, Fernandez A, Borge-Holthoefer J and Arenas A Radatools 3.2—Communities detection in complex networks and other tools http://deim.urv.cat/~sergio.gomez/radatools.php

[35] Kuncheva L I and Hadjitodorov S T 2004 Using diversity in cluster ensembles *IEEE Intl Conf. on Systems, Man and Cybernetics* **2** 1214–9

[36] Fred A L N and Jain A K 2003 Robust data clustering *Proc. IEEE Computer Society Conf. on Computer Vision and Pattern Recognition* vol 2 (IEEE) pp II–128

[37] Goh K-I, Kahng B and Kim D 2001 Universal behavior of load distribution in scale-free networks *Phys. Rev. Lett.* **87** 278701

[38] Wasserman S and Galaskiewicz J 1994 *Advances in Social Network Analysis: Research in the Social and Behavioral Sciences* vol 171 (Thousand Oaks, CA: Sage Publications)

[39] Zhou S and Mondragón R J 2004 The rich-club phenomenon in the internet topology *IEEE Commun. Lett.* **8** 180–2

[40] van den Heuvel M P and Sporns O 2011 Rich-club organization of the human connectome *J. Neurosci.* **31** 15775–86

[41] Harriger L, van den Heuvel M P and Sporns O 2012 Rich club organization of macaque cerebral cortex and its role in network communication *PloS ONE* **7** e46497

[42] Varshney L R, Chen B L, Paniagua E, Hall D H and Chklovskii D B 2011 Structural properties of the caenorhabditis elegans neuronal network *PLoS Comput. Biol.* **7** e1001066

[43] Chen B L, Hall D H and Chklovskii D B 2006 Wiring optimization can relate neuronal structure and function *Proc. Natl. Acad. Sci. USA* **103** 4723–8

[44] Traxl D 2012 *C. elegans*—Neural structure & dynamics *Master's Thesis* Ludwig-Maximilians-Universität München

[45] Schafer W R 2005 Deciphering the neural and molecular mechanisms of *C. elegans* behavior *Curr. Biol.* **15** 723–9

[46] Scannell J W, Burns G A P C, Hilgetag C C, O'Neil M A and Young M P 1999 The connectional organization of the cortico-thalamic system of the cat *Cerebral Cortex* **9** 277–99

[47] Hagmann P, Cammoun L, Gigandet X, Meuli R, Honey C J, Wedeen V J and Sporns O 2008 Mapping the structural core of human cerebral cortex *PLoS Biol.* **6** e159

[48] Lew J M, Kapopoulou A, Jones L M and Cole S T 2011 Tuberculist-10 years after *Tuberculosis* **91** 1–7

[49] Damasio A R 1989 Time-locked multiregional retroactivation: a systems-level proposal for the neural substrates of recall and recognition *Cognition* **33** 25–62

[50] Bressler S L and Kelso J A S 2001 Cortical coordination dynamics and cognition *Trends Cogn. Sci.* **5** 26–36

[51] Fuster J M 2003 *Cortex and Mind: Unifying Cognition* (Oxford: Oxford University Press)

[52] Shanahan M 2007 A spiking neuron model of cortical broadcast and competition *Consciousness Cogn.* **17** 288–303

[53] Bartsch R P and Ivanov P C 2014 Coexisting forms of coupling and phase-transitions in physiological networks *Commun. Comp. Inf. Sci.* **438** 270–87

[54] Kivelä M, Arenas A, Barthelemy M, Gleeson J P, Moreno Y and Porter M A 2014 Multilayer networks *J. Complex Networks* **2** 203–71

[55] Mucha P J, Richardson T, Macon K, Porter M A and Onnela J-P 2010 Community structure in time-dependent, multiscale, and multiplex networks *Science* **328** 876–8

[56] Schaub M T, Lambiotte R and Barahona M 2012 Encoding dynamics for multiscale community detection: Markov time sweeping for the map equation *Phys. Rev.* E **86** 026112

[57] Arenas A, Fernández A and Gómez S 2008 A complex network approach to the determination of functional groups in the neural system of *C. elegans Bio-Inspired Computing and Communication* (New York: Springer) pp 9–18

[58] Lohse C, Bassett D S, Lim K O and Carlson J M 2014 Resolving anatomical and functional structure in human brain organization: Identifying mesoscale organization in weighted network representations *PLoS Comput. Biol.* **10** e1003712

[59] Sanz J, Cozzo E, Borge-Holthoefer J and Moreno Y 2012 Topological effects of data incompleteness of gene regulatory networks *BMC Syst. Biol.* **6** 110